

1 **Revised text following**

2 **REVISION #1**

3

4

Text word count 3511

5 **The "breathing" Earth (la terra che respira) at Solfatara-Pisciarelli (Campi Flegrei,**
6 **southern Italy) during 2005-2024: Nature's way of attenuating the effects of**
7 **bradyseism through gradual and episodic release of subsurface pressure.**

8 **Lima A.¹, Bodnar R.J.², De Vivo B.³, Spera F.J.⁴ and Belkin H.E.⁵**

9

10 ¹Dipartimento di Scienze della Terra, dell'Ambiente e delle Risorse (DiSTAR), Università di Napoli Federico II,
11 Complesso Universitario di Monte Sant'Angelo, Via Cintia 26, 80126 Napoli, Italy

12 ²Department of Geosciences, Virginia Tech, 4044 Derring Hall, Blacksburg, Virginia 24061, USA

13 ³Università di Napoli Federico II, Italy (Retired); Adjunct Prof.at: Virginia Tech, Blacksburg, USA and Nanjing Univ.,
14 Nanjing, China, Via Belsito 17, 80125 Napoli, Italy.

15 ⁴Department of Earth Science and Earth Research Institute, University of California, Santa Barbara, CA, USA 93106

16 ⁵U. S. Geological Survey (Retired), 11142 Forest Edge Dr., Reston, Virginia 20190, USA

17

18 **Abstract**

19 Campi Flegrei (CF) is a large volcanic complex west of Naples, in a densely populated region at high
20 volcanic risk due to recurrent ground uplift and subsidence (bradyseism) that has been ongoing since at
21 least Greek-Roman times. We compare the current period of unrest beginning in 2005 with that of the
22 bradyseism crisis of 1982-84. Despite the similarity in the quasi-radially symmetric pattern of ground
23 deformation suggesting a similar source location and overpressure, the current uplift rate is about 8 times
24 lower, and the seismic release energy is an order of magnitude lower than in 1982-84, and mainly located
25 in isolated regions below the Solfatara-Pisciarelli area. We interpret the recent earthquake swarms at
26 Solfatara-Pisciarelli as a reflection of the activation of a fault system that was inactive during previous
27 bradyseism crises. Furthermore, the increase of Solfatara-Pisciarelli fumarole mass flux is the
28 manifestation of fluid discharge that significantly reduces the uplift rate of the ongoing bradyseism event.
29 As a result, the effects of bradyseism in the CF system have self-attenuated through increased fluid
30 expulsion ("*breathing or exhalation*") from the deep lithostatically-pressured reservoir. Having gained a
31 clear understanding of the causes of bradyseism at CF, we suggest that modern geoen지니어링
32 approaches developed to exploit high-temperature geothermal reservoirs may be employed to manage

33 fluid flow and reduce the pressure exerted by geothermal fluids in the Solfatara-Pisciarelli area with the
34 aim of minimizing the risk of phreatic eruptions and, concomitantly, reducing uplift and seismicity. This
35 approach requires concerted and cooperative efforts between geoscientists, engineers, government
36 officials, and the general public.

37 **1. OVERVIEW OF THE CF VOLCANIC SYSTEM**

38 Lima et al. (2021) previously described the “bradyseism signature” at Campi Flegrei (CF) as the
39 ensemble of cyclical phenomena associated with ground deformation. CF is an area of very high volcanic
40 risk, and it is therefore critical to be able to distinguish between uplift or deformation that may be a
41 precursor to an eruption, as occurred in 1538 preceding the Monte Nuovo event, and ground deformation
42 showing the “bradyseism signature” and which does not presage an eruption. The unrest at CF beginning
43 in 2005 and continuing today shows a typical "bell shaped" spatial pattern of ground deformation (Fig. 1)
44 in which the magnitude of uplift and subsidence decay rapidly with distance from the central location of
45 maximum uplift/subsidence, with the epicenter located at the town of Pozzuoli.

46 De Vivo and Lima (2006) noted that the magmatic and hydrothermal systems at CF are similar to those
47 associated with formation of porphyry copper deposits. In subsequent years, quantitative conceptual
48 models were developed (Bodnar et al., 2007, Lima et al., 2009; 2021) to show that bradyseism could be
49 related to the transition from magmatic to hydrothermal conditions in a subvolcanic environment based on
50 the model of Fournier (1999). The subsurface at CF is composed of three fluid reservoirs, separated by
51 two relatively impermeable horizons. The deepest reservoir contains magmatic fluids (mostly CO₂ and
52 H₂O) generated by exsolution from a deeper magma body as it cools, crystallizes and expels fluid. The
53 fluids in this deep reservoir are separated from those in the overlying hydrothermal reservoir by the
54 relatively impermeable crystallized outer portion of the magma body (layer A; Fig. 2A) that Burnham
55 (1979) refers to as the "crystallized rind". Episodically, impermeable layer A fractures, allowing
56 magmatic fluids to migrate into the overlying reservoir (Fig. 2B). A critical component of bradyseism at
57 CF is the presence of a second impermeable layer B (claystone/siltstone cap; Fig.2) that separates and

58 maintains the deeper hydrothermal system without substantial variations for centuries (Vanorio and
59 Kanitpanyacharoen, 2015). As such, impermeable layer B acts as a throttling valve between the deep
60 hydrothermal system and the shallow hydrostatically-pressured aquifer. This valve operates on short time
61 scales ($1-10^2$ years) decoupled from the longer timescale associated with magma cooling, crystallization,
62 and fluid expulsion. The valve cyclicality (open vs. shut) causes conditions in the deeper reservoir to
63 alternate between lithostatic and hydrostatic pressure (Fig. 2A and 2C). Connectivity between the shallow
64 hydrostatic and deeper lithostatic reservoirs is episodically turned on and off, perhaps related to cycles of
65 deposition from hydrothermal solutions (permeability decrease) and new phases of fracture formation
66 (permeability increase), causing alternating periods of uplift and subsidence, depending on the temporal
67 evolution of the permeability field and associated thermo-poroelasticity of the host rocks. Earthquake
68 swarms are the manifestation of formation of hydrofractures in the impermeable layer. These fractures
69 allow fluid decompression and expansion, transport and mineral (e.g., silica) precipitation that leads to
70 sealing of cracks and isolation of the two reservoirs (Fig. 2D).

71 Thus, pressure slowly builds up within the hydrothermal reservoir beneath impermeable layer B (Fig.
72 2) until the pressure is reduced by permeability increase due to fracture propagation concomitant with the
73 expulsion of fluids from the deeper reservoir into the shallower one. The processes operating in the
74 subsurface at CF are not unlike those responsible for the regular eruptions of Old Faithful Geyser in
75 Yellowstone National Park, USA, whereby constrictions (i.e., permeability barriers) in the deep plumbing
76 system prevent water from moving from depth to the surface until sufficient pressure builds up to allow
77 water to pass through the constrictions and escape to the surface.

78 The seismogenic zone at CF is bounded by two impermeable layers. The shallower one (layer B in Fig.
79 2) has greater elasticity (Vanorio and Kanitpanyacharoen, 2015; Ahmed, 2018; Sayed et al., 2018; Heap
80 et al., 2020) compared to the deeper one (Layer A in Fig. 2). Additionally, fault systems around the lateral
81 margins are truncated by an anticline that allows the hydrothermal system to be preserved without

82 variation for millennia. Danesi et al. (2024) generally confirm this pattern through a detailed study of
83 seismic data recorded during the period 1982-2023.

84 The current period of bradyseism unrest began in 2005. However, despite the commonality of the
85 quasi-radial symmetric pattern of ground deformation, suggesting a similar source location and
86 overpressure, the uplift rate, the spatial distribution of seismicity, and the seismic energy release show
87 quantitatively significant differences for the two periods (1982-84 and 2005-24). For the current unrest,
88 the uplift rate is about 8 times slower than in 1982-84, and earthquakes below the point of maximum
89 uplift and the released seismic energy are an order of magnitude smaller than in 1982-84 and mainly
90 located in isolated regions below the Solfatara-Pisciarelli area (Tramelli et al., 2022; Danesi et al., 2024).

91 **2. EVOLUTION IN INTERPRETATION OF CAUSES OF BRADYSEISM AT CF**

92 Various models have been put forward to explain the bradyseism at CF (see also Lima et al., 2021) and
93 they can be divided into three groups. The first group of models interprets CF unrest to be the result of
94 intrusion of magmas to shallow depths of ~3 km, such that input of new magma in the subsurface leads to
95 deformation at the surface (e.g., Woo and Kilburn, 2010, Amoruso and Crescentini, 2011). Through
96 analysis of deformation and microgravity data, parameters characterizing the magmatic source, such as
97 shape, petrophysical properties (rigidity modulus, Poisson's ratio) the change in volume and hence
98 pressure are estimated. These models fail to explain subsequent subsidence that always follows an uplift
99 phase. In fact, uplift induced by a magmatic intrusion varies very little over short (on the order of a year)
100 timescales. The timescale of a magmatic event is quite long since magma volume is not removed (no
101 eruptions before, during or after recent bradyseism crises). The explanation of the 80 cm of subsidence
102 that occurred in the subsequent 20 years following the 1982-1984 unrest (Del Gaudio et al., 2010) is
103 better explained by the implications of the cyclic model and related thermo-poroviscoelastic effects that
104 accompany the movement of crustal fluids.

105 The second set of models relate uplift to magmatic intrusions but additionally focuses on developing
106 more convincing explanations for the subsidence that invariably follows (e.g. Troise et al., 2019; Chiodini

107 et al., 2021; Giacomuzzi et al., 2024). The subsidence is generally interpreted due to hydrothermal
108 processes in the subsurface, but a detailed explanation of how the transition from uplift to subsidence
109 occurs is not provided. During unrest the involvement of shallow magma intrusions is based on the
110 decreasing H₂O/CO₂ ratio in the Solfatara volcano fumaroles as a result of addition of magmatic CO₂ to
111 the fumaroles (Chiodini et al., 2015). Recently, Giacomuzzi et al. (2024) concluded that evidence for the
112 presence of magma bodies at shallow depths is lacking, based on a detailed seismic tomography analysis.

113 The third group of models explains unrest at CF to be the result of hydrothermal fluid migration in
114 three intermittently isolated fluid reservoirs, as discussed above (see Fig. 2), with *no* addition of new
115 magma to the magma body at depth. The latter hydrothermal model works well for the interpretation of
116 bradyseism and has been supported by more recent studies asserting that magmatic intrusions are not
117 required to explain bradyseism. These workers (e.g. Nespoli et al., 2021; 2023) apply a physical model
118 that considers that a Thermo-Poro-Elastic (TPE) inclusion, with an assigned geometry, is responsible for
119 deformation induced by mechanical effects of both pore pressure and temperature changes of the fluids
120 which pervade a poroelastic region, embedded in an elastic matrix. Based on tomography studies, layer B
121 (Fig. 2) with time dependent permeability below the shallow aquifer has been recognized (e.g., Calò and
122 Tramelli, 2018; Nespoli et al., 2021; Danesi et al., 2024) to play an important role in bradyseismic events.
123 Vanorio and Kanitpanyacharoen (2015) stress the importance of the claystone/siltstone impermeable layer
124 that acts as a caprock affording the capability to accommodate the strain as fluids accumulate and pore
125 fluid pressure increases until a critical threshold is exceeded.

126 The models that ascribe bradyseism to be the result of shallow magmatic intrusions cannot explain the
127 repetitive cyclical signals without substantial variations over time, as well as the constancy of the
128 seismogenic volume during a bradyseismic episode. The maximum uplift is always centered at Pozzuoli.
129 In addition, the results of both seismic tomography (Zollo et al., 2008; Calò and Tramelli, 2018;
130 Giacomuzzi et al., 2024) and the density model built using a new 3-D inversion of the available high-

131 precision gravity and deformation data (Amoruso et al., 2008; Capuano et al., 2013; Amoruso and
132 Crescentini, 2022) also exclude the presence of magma at shallow levels.

133 3. WHAT IS THE DRIVING FORCE OF BRADYSEISM AT CF?

134 The ultimate heat engine that drives bradyseism at CF is the deep magmatic system at >7.5 km depth.
135 The surrounding deep fluid environment proximal to the cooling magma body is similar to that
136 documented in magmatic-hydrothermal ore deposit systems associated with porphyry copper deposits
137 (e.g., Burnham, 1979; Fournier, 1999; Becker et al., 2019) (Fig.2). *Bradyseism is a cyclical phenomenon*
138 *that can last for millennia and is not a precursor to a volcanic eruption because it is driven by the*
139 *transient connection between the deeper lithostatic reservoir and an overlying more permeable*
140 *hydrostatic one, and does not require new magma to have been added to the deeper magmatic system.* In
141 the magmatic-hydrothermal model of Lima et al. (2021), the ultimate driver of bradyseism includes heat
142 and fluid from the deeper reservoir; the addition of magma from the very deep crust or mantle to shallow
143 depth is *not* an integral feature. Indeed, the mechanism proposed is driven by the geothermal environment,
144 and is not dependent on addition of new magma.

145 In the hydrothermal model two different processes operate - each at a unique timescale; one is the 10^4 - 10^5
146 years timescale associated with magma solidification (and associated magmatic fluid generation and
147 expulsion) (Ingebritsen et al., 2010; Cox et al., 2001). During this long timescale process the brittle-ductile
148 transition migrates downward as magma cools and crystallizes (see Becker et al. 2019, their Fig. 2). The
149 second shorter timescale (1 - 10^2 years) is intrinsically episodic and associated with fluid migration and
150 concomitant transient fracture propagation events that compromise the mechanical integrity of layer B,
151 connecting the lower lithostatic reservoir with the upper hydrostatic one (Fig. 2B and 2C). Connectivity
152 between the reservoirs is enhanced or is dampened by opening of fractures to increase permeability or by
153 mineral precipitation (e.g., deposition of silicates, sulfates, carbonates, and sulfides) and, hence,
154 permeability decrease (Fig. 2D). The pervasive zoning of the epidote supergroup minerals observed in

155 drill cores records the episodic nature of hydrofracturing and the pulsing of geothermal fluids (Belkin and
156 De Vivo, 2023).

157 When a hydrous melt becomes saturated in H₂O and exsolves a magmatic H₂O phase, the volume of
158 the system (crystals + melt + fluid) increases significantly at constant pressure. At pressures of 100-200
159 MPa, the system volume change can be 50% or greater, and even at 0.6 GPa (roughly 20 km depth) the
160 volume of the system (crystals + melt + H₂O) will increase by about 10% (Burnham, 1972, 1985), owing
161 to the large difference between the partial molar volume of H₂O in the melt compared to the molar
162 volume of the separated magmatic H₂O phase. If the system is unable to expand to accommodate the
163 volume increase (as in the case of magma that is surrounded by impermeable and rigid crystallization
164 products), pressure increases. In an isochoric process, large amounts of mechanical energy are stored in
165 the magma chamber (Fig. 3). This energy leads eventually to fracturing (via hydrofracturing) allowing the
166 magmatic aqueous phase and, in some cases, magma, to escape into the overlying rocks (Bodnar et al.,
167 2007; Lima et al., 2009; Lima et al., 2021). The decrease in H₂O /CO₂ ratio of fumarolic fluids (Chiodini
168 et al., 2015; 2021) is interpreted to represent addition of magmatic CO₂ to the hydrothermal system and
169 indicates that fluids do indeed escape. Because the magmatic fluids expelled are quite hot, a sharp
170 temperature front is present and migrates at a speed on the order of Darcy flow rate of order $v \sim \frac{\rho_f K g \alpha_f \Delta T}{\eta}$
171 where ρ_f , K , g , α_f , ΔT , and η represent the fluid density, permeability, acceleration due to gravity, fluid
172 isobaric expansivity, characteristic temperature difference between upper and lower reservoirs and fluid
173 viscosity, respectively. Adopting typical values for H₂O at 0.1 GPa (~3 km depth) and 400 °C (Haar et al.,
174 1984) of 693 kg/m³, 10⁻³ K⁻¹, and 8x10⁻⁵ Pa s for density, expansivity and viscosity, respectively, and
175 setting $\Delta T = 400$ K and $K = 10^{-13}$ m² gives a percolation (Darcy) velocity of $v \approx 110$ m/year. This
176 shows that ground deformation takes place on a timescale consistent with observed uplifts of a few years
177 and not on the magmatic timescale on the order of many thousands of years. Quantitatively, Bonafede
178 (1991) has noted the thermo-poroelastic deformation associated with the advection of superheated steam

179 can easily provide uplifts on the order of 1 meter on a short timescale, consistent with observations.
180 Finally, it is noted that if fluid escape is very efficient, the volume change associated with magma
181 crystallization is negative since solid (crystals), being denser, occupies less volume than melt and
182 detumescence (collapse) rather than tumescence (uplift) occurs. The value of permeability (10^{-13} m^2) used
183 to determine the above characteristic Darcy velocity is a mean value typical of geothermal areas (e.g.,
184 Nield and Bejan, 1992). However, on shorter spatial and time scales precipitation and/or dissolution of
185 hydrothermal phases due to decompression and cooling of expelled fluids will ensure a complex
186 permeability field that evolves both spatially and temporally, a topic for future work.

187 **4.WHY IS THE RECENT UPLIFT RATE SLOWER THAN THAT IN 1982-1984?**

188 The current unrest shows an uplift rate that is about 8 times lower than in 1982-84, and the seismically
189 released energy, located in a restricted region below the Solfatara-Pisciarelli area (Danesi et al., 2024), is
190 an order of magnitude lower than in 1982-84. As discussed above, if the CF magmatic-hydrothermal
191 system is completely closed, the mechanical energy associated with magma crystallization (Fig. 3) would
192 be capable of generating a maximum uplift of 40 m (Lima et al., 2009). It is very unlikely that a natural
193 system such as CF that is extensively fractured including numerous lateral faults (Capuano et al., 2013)
194 could be closed with respect to fluid loss. Indeed, the presence of active fumaroles and hot springs in the
195 region (Scotto di Uccio et al., 2024) is *prima facie* evidence for open system behavior. When fluid is
196 allowed to escape, the amount of uplift is reduced in proportion to the amount of fluid leakage from the
197 deep reservoir, recharged by fluids that are exsolving from the magma (second boiling). Chiodini et al.
198 (2015; 2021) highlighted that fumarolic activity in the Solfatara-Pisciarelli area (Fig. 1) since 2005 has
199 significantly increased, with fumarolic gases showing the presence of elements and compounds of
200 magmatic origin, such as CO_2 . This is consistent with the advection of hot fluids and associated thermo-
201 poroelastic deformation discussed above. In addition, Danesi et al. (2024) show that seismicity occurred
202 west of Solfatara in 2005-2023, with the cluster of events developing at depths of 2-3 km beneath

203 Solfatara starting in 2005, with clusters of shallow earthquakes extending from depths of 0.5-1 km toward
204 Pisciarelli.

205 The current uplift rate can be interpreted to reflect the activation of a fault system in the Solfatara-
206 Pisciarelli area (Scotto di Uccio et al., 2024) that allows the CF hydrothermal system to discharge energy
207 by escape of fluids and preventing the buildup of high poro-elastic pressures and associated enhanced
208 ground deformation. In previous bradyseism crises these fractures were not active (Danesi et al., 2024),
209 and uplift was greater than in the current crisis. This is the only difference between the former and present
210 bradyseism events so far recorded. The cyclic nature of the ongoing bradyseism is closely related to the
211 complex geological, tectonic, and stratigraphic upper crustal structures that govern spatial and temporal
212 variations of the subsurface permeability and distribution of fluid pressure associated with migration of
213 fluids. Earthquake swarms in the Solfatara-Pisciarelli area and the increase of fumarole outflows are the
214 manifestation of enhanced fluid discharge (compared to 1982-84) from the hydrothermal reservoir
215 contained between impermeable layers A and B that significantly reduces the uplift rate of the ongoing
216 bradyseism event.

217 The rate of subsidence is a function of the extent of brecciation (fracturing) of the impermeable layer
218 B. The extent of fracturing does not represent a competition between fluid escape and injection rates
219 because the release of magmatic fluid is continuous over time. In the shallow hydrothermal reservoir,
220 seawater and meteoric water can mix with the magmatically-derived fluids intermittently, thereby
221 introducing another layer of complexity. In 1985 (Fig. 2C), extensive fracturing of the impermeable
222 barrier occurred, and subsidence resulted. In the immediate future, it is much more likely that the uplift
223 will continue for some years at a rate that can vary depending on the efficiency of fluid discharge at
224 Solfatara Pisciarelli. Thus, in a completely natural way, the CF system is "*breathing*" and has self-
225 attenuated the effects of bradyseism.

226 **5.IMPLICATIONS**

227 Having gained an understanding of the processes that lead to bradyseism at CF - that is, the rate and
228 extent of uplift and subsidence is controlled by a natural valve system at depth that is represented by
229 impermeable layer B (Fig. 2) as well as the presence of subsurface conduits (faults) that allow fluids to
230 migrate laterally. As such, it may be possible to control the flow of fluids in the Solfatara-Pisciarelli area
231 with the aim of minimizing future periods of ground deformation and seismicity. By drilling boreholes
232 that penetrate impermeable layer B, high permeability zones that allow continuous transfer of fluids from
233 the deeper to more shallow reservoirs can be introduced. As such, pressure would not build up (or, at
234 least, the extent of pressure build up would be reduced) beneath layer B and thermo-elastic deformation
235 would be limited. Targeted pumping of subsurface fluids would facilitate drainage of the system and
236 minimize hydrofracturing and seismic activity in general. Considering that the input of rainwater
237 increases seismic tremor activity (Scafetta and Mazzarella, 2021), it is clear how important drainage is in
238 the surface aquifer as well.

239 The geothermal industry has demonstrated that it is possible to drill geothermal wells to at least 5,000
240 m and to temperatures up to 500°C (Rivera and Carey, 2023) including operations in supercritical
241 geothermal systems (Reinsch et al., 2017). Drilling deep geothermal wells can be accomplished at a cost
242 that is much less than the cost of damage, and risk to human health and safety, associated with periods of
243 unrest at CF. In the 1970-80s, numerous boreholes were drilled in CF to explore for geothermal resources
244 (Fig. 1). For example, well SV1 reached a total depth of 3,040 m (AGIP, 1987; De Vivo et al., 1989). The
245 risk linked to drilling can be managed with modern technologies that have been developed to exploit very
246 high temperature ($\leq 500^{\circ}\text{C}$) geothermal reservoirs (c.f., Rivera and Carey, 2023), and the proposed
247 objectives would not require the re-location of residents of CF. Bradyseism could be managed and
248 controlled by careful geoengineering. In any case, concerted efforts are needed to bring together
249 geoscientists, engineers, government officials, and the general public to address and solve this ongoing
250 problem using existing knowledge and tools. Through dedicated efforts it is possible to manage the forces

251 of nature, and with a cost/benefit ratio that is very favorable for the many thousands of people living
252 within the CF volcanic complex.

253

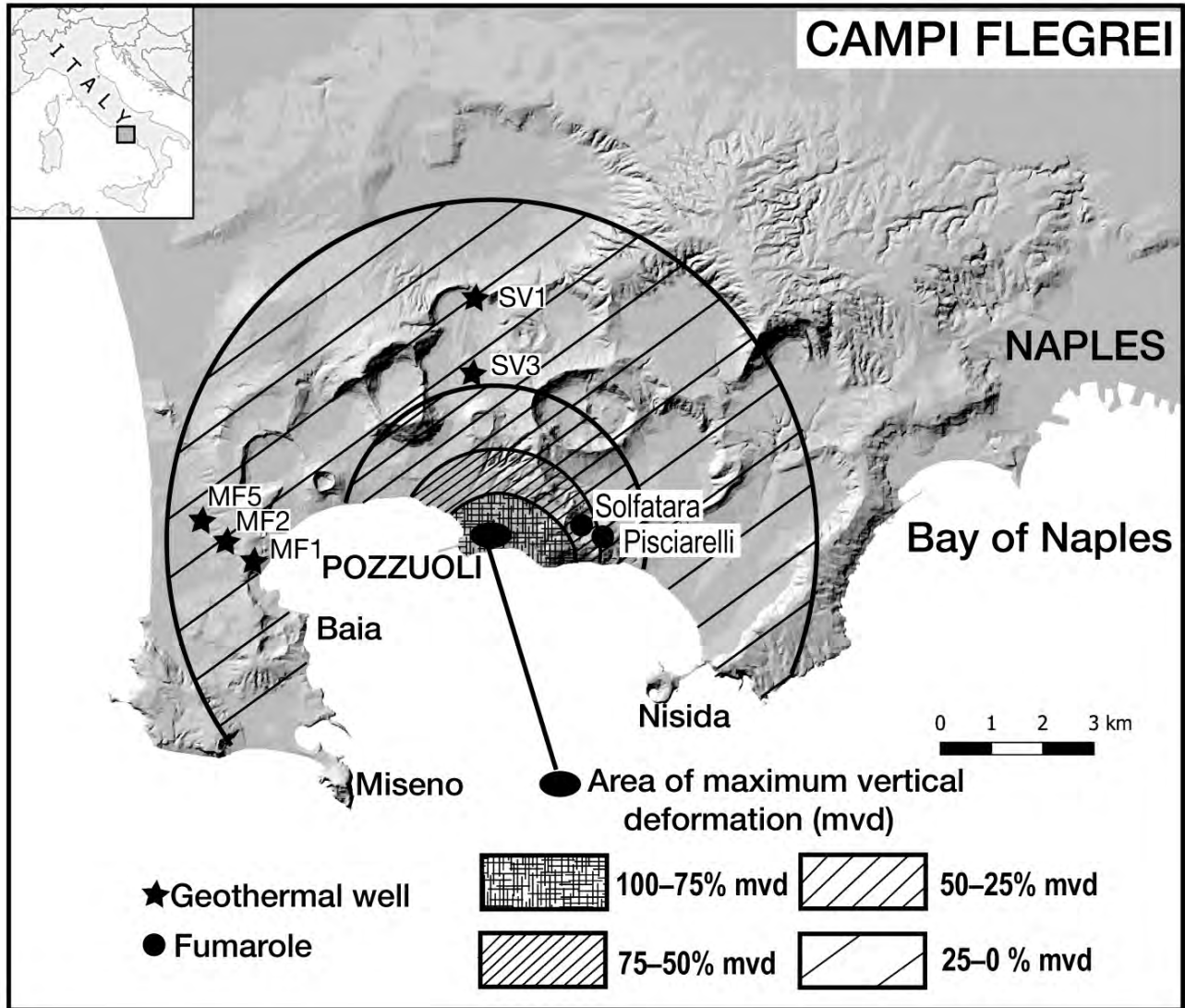
254 **References**

- 255 AGIP (1987). Geologia e geofisica del sistema geotermico dei Campi Flegrei, Internal Report, Milan, Italy.
- 256 Ahmed S.M. (2018). Assessment of clay stiffness and strength parameters using index properties, Journal of Rock Mechanics
257 and Geotechnical Engineering, V10, 3, 579-593, <https://doi.org/10.1016/j.jrmge.2017.10.006>.
- 258 Amoruso, A., Crescentini L., and Berrino, G. (2008). Simultaneous inversion of deformation and gravity changes in
259 horizontally layered half-space: evidences for magma intrusion during the 1982–1984 unrest at Campi Flegrei caldera
260 (Italy). Earth and Planetary Science Letters, 272, 181-188. <https://doi.org/10.1016/j.epsl.2008.04.040>.
- 261 Amoruso, A., and Crescentini, L. (2011). Modelling deformation due to a pressurized ellipsoidal cavity, with reference to the
262 Campi Flegrei Caldera, Italy. Geophysical Research Letters, <https://doi.org/10.1029/2010GL046030>.
- 263 Amoruso, A., and Crescentini, L. (2022). Clues of ongoing deep magma inflation at Campi Flegrei Caldera (Italy) from
264 empirical orthogonal function. Anal. SAR Data Remote Sens 14.
- 265 Becker, S.P., Bodnar, R.J., and Reynolds, T.J. (2019). Temporal and spatial variations in characteristics of fluid inclusions in
266 epizonal magmatic-hydrothermal systems: Applications in exploration for porphyry copper deposits. Journal of
267 Geochemical Exploration, 204, 240-255. <https://doi.org/10.1016/j.gexplo.2019.06.002>.
- 268 Belkin, H.E., and De Vivo, B. (2023). Compositional variation and zoning of epidote supergroup minerals in the Campi Flegrei
269 geothermal field, Naples, Italy. European Journal of Mineralogy, 35, 25-44. Doi: 10.5194/ejm-35-25-2023.
- 270 Bodnar, R.J., Cannatelli, C., De Vivo, B., Lima, A., Belkin, H.E., and Milia, A. (2007). Quantitative model for magma
271 degassing and ground deformation (bradyseism) at Campi Flegrei, Italy: implications for future eruptions. Geology, 35(9):
272 791-794. doi: 10.1130/G23653A.1.
- 273 Bonafede, M. (1991). Hot fluid migration: an efficient source of ground deformation: application to the 1982-1985 crisis at
274 Campi Flegrei-Italy. In: G. Luongo and R. Scandone (Eds). Journal of Volcanology and Geothermal Research, 48, 187-198.
- 275 Burnham, C.W. (1972). The energy of explosive volcanic eruptions. Earth Mineral Sciences. The Pennsylvania State
276 University, 41, 69-70.
- 277 Burnham, C.W. (1979). Magmas and hydrothermal fluids. 71-136. In: Barnes H. L., Editor, Geochemistry of hydrothermal ore
278 deposits, 2nd Edition, 71-136, John Wiley & Sons, New York, 1979, 798 pp.
- 279 Burnham, C.W. (1985). Energy release in subvolcanic environments: implications for breccia formation. Economic Geology,
280 80, 1515-1522.
- 281 Calò, M., and A., Tramelli (2018). Anatomy of the Campi Flegrei caldera using enhanced seismic tomography models,”
282 Scientific Reports, vol. 8, no. 1, p. 16254.

- 283 Capuano P., Russo G., Civetta L., Orsi G., D'Antonio M., and Moretti, R. (2013). The active portion of the Campi Flegrei
284 caldera structure imaged by 3-D inversion of gravity data. *Geochemistry, Geophysics, Geosystems*, vol. 14, no. 10, pp.
285 4681-4697.
- 286 Chiodini, G., Vandemeulebrouck, J., Caliro, S., D'Auria L., De Martino, P., Mangiacapra, A., and Petrillo, Z. (2015). Evidence
287 of thermal-driven processes triggering the 2005-2014 unrest at Campi Flegrei caldera. *Earth and Planetary Science Letters*,
288 414, 58-67.
- 289 Chiodini, G., Caliro, S., Avino, R., Bini, G., Giudicepietro, F., Cesare, W.D., Ricciolino, P., Aiuppa, A., Cardellini, C., Petrillo,
290 Z., Selva, J., Siniscalchi, A., and Tripaldi, S. (2021). Hydrothermal pressure-temperature control on CO₂ emissions and
291 seismicity at Campi Flegrei (Italy). *Journal of Volcanology and Geothermal Research* 107245 [https://doi.org/10.1016/j.](https://doi.org/10.1016/j.jvolgeores.2021.107245)
292 [jvolgeores.2021.107245](https://doi.org/10.1016/j.jvolgeores.2021.107245).
- 293 Cox, S. F., Knackstedt, M. A. and Braun J., 2001. Principles of Structural Control on Permeability and Fluid Flow in
294 Hydrothermal Systems. In: *Structural Controls on Ore Genesis*, (Jeremy P. Richards, Richard M. Tosdal, eds.). *Reviews in*
295 *Economic Geology*, 14, <https://doi.org/10.5382/Rev.14.01>.
- 296 Danesi, S., Pino, N.A., Carlino, S., and Kilburn, C.R.J. (2024). Evolution in unrest processes at Campi Flegrei caldera as
297 inferred from local seismicity. *Earth and Planetary Science Letters*, 626,, 118530, doi.org/10.1016/j.epsl.2023.118530.
- 298 Del Gaudio, C., Aquino, I., Ricciardi, G.P., Ricco C, and Scandone, R. (2010). Unrest episodes at Campi Flegrei: A
299 reconstruction of vertical ground movements during 1905-2009, *Journal of Volcanology and Geothermal Research*, ~~vol.~~
300 195, 48–56.
- 301 De Vivo, B., Belkin, H.E., Barbieri, M., Chelini, W., Lattanzi, P., Lima, A., and Tolomeo, L. (1989). The Campi Flegrei (Italy)
302 geothermal system: A fluid inclusion study of the Mofete and San Vito fields. *Journal of Volcanology and Geothermal*
303 *Research*, 36, 303-326.
- 304 De Vivo B., and Lima, A. 2006. A hydrothermal model for ground movements (bradyseism) at Campi Flegrei, Italy. In:
305 *Volcanism in the Campania Plain: Vesuvius, Campi Flegrei and Ignimbrites* (De Vivo B., ed). *Developments in*
306 *Volcanology* 9, Elsevier, p. 289-317.
- 307 Fournier, R.O. (1999). Hydrothermal processes related to movement of fluid from plastic into brittle rock in the magmatic-
308 epithermal environment. *Economic Geology*, 94 (8), 1193-1212.
- 309 Giacomuzzi, G., Chiarabba, C., Bianco, B., De Gori, P., and Piana Agostinetti, N. (2024). Tracking transient changes in the
310 plumbing system at Campi Flegrei Caldera, *Earth and Planetary Letters*, 637, <https://doi.org/10.1016/j.epsl.2024.118744>
- 311 Haar, L., Gallagher, J.S., and Kell, G.S. (1984). *NBS/NRC Steam Tables*. Hemisphere Publishing Corporation, Washington,
312 DC.

- 313 Heap, M..J., Villeneuve, M., Albino, F., Farquharson, J.I., Brothelande, E., Amelung, F., Got, J.L., and Baud, P. (2020).
314 Towards more realistic values of elastic moduli for volcano modelling, *Journal of Volcanology and Geothermal Research*,
315 390, 106684, <https://doi.org/10.1016/j.jvolgeores.2019.106684>.
- 316 Ingebritsen, S.E., Geiger, S., Hurwitz, S., and Driesner, T. (2010). Numerical simulation of magmatic hydrothermal systems,
317 *Rev. Geophys.*, 48, RG1002, doi:10.1029/2009RG000287.
- 318 Lima, A., De Vivo, B., Spera, F.J., Bodnar, R.J., Milia, A., Nunziata, C., Belkin, H.E., and Cannatelli, C. (2009).
319 Thermodynamic model for the uplift and deflation episodes (bradyseism) associated with magmatic-hydrothermal activity
320 at the Campi Flegrei active volcanic center (Italy). *Earth Science Review*, 97, 44-58. Doi: 10.1016/j.earscirev.2009.10.001.
- 321 Lima, A., Bodnar, R. J., De Vivo, B., Spera, F. J., and Belkin, H. E. (2021). Interpretation of recent unrest events (bradyseism)
322 at Campi Flegrei, Napoli (Italy): Comparison of models based on cyclical hydrothermal events versus shallow magmatic
323 intrusive events. *Geofluids*, ID 2000255 Doi: 10.1155/2021/2000255
- 324 Nespoli, M., Belardinelli, M.E., and Bonafede, M. (2021). Stress and deformation induced in layered media by cylindrical
325 thermo-poro-elastic sources: an application to Campi Flegrei (Italy). *Journal of Volcanology and Geothermal Research*,
326 415, 107269. <https://doi.org/10.1016/j.jvolgeores.2021.107269>.
- 327 Nespoli, M., Belardinelli, M.E., and Bonafede, M. (2023). Thermo-poro-viscoelastic response of a disc-shaped inclusion.
328 *Geophysical Journal International*, 235, 135-149, doi: 10.1093/gji/ggad212.
- 329 Nield, D. A., and Bejan, A. (1992). Convection in porous media. <https://api.semanticscholar.org/CorpusID:201328542>
- 330 Reinsch, T., Dobson, P., Asanuma, H., Huenges, E., Poletto, F., and Sanjuan, B. (2017). Utilizing supercritical geothermal
331 systems: 625 a review of past ventures and ongoing research activities, *Geothermal Energy*, 5, 16,
332 <https://doi.org/10.1186/s40517-017-0075-y>.
- 333 Rivera, J., and Carey, B.S., (2023). Comparative geothermal well performance-supercritical and subcritical. *GNS Science*
334 *Report 2023/01*.
- 335 Sayed S.M. (2018). Assessment of clay stiffness and strength parameters using index properties, *Journal of Rock Mechanics*
336 *and Geotechnical Engineering*, V10, 3, 579-593, <https://doi.org/10.1016/j.jrmge.2017.10.006>.
- 337 Scafetta, N., and Mazzarella, A. (2021). On the rainfall triggering of Phlegraean Fields volcanic tremors. *Water*, 13 (2), 154;
338 <https://doi.org/10.3390/w13020154>
- 339 Scotto di Uccio, F., Lomax, A., Natale, J., Muzellec, T., Festa, G., Nazeri, S., et al. (2024). Delineation and fine-scale structure
340 of fault zones activated during the 2014–2024 unrest at the Campi Flegrei caldera (Southern Italy) from high-precision
341 earthquake locations. *Geophysical Research Letters*, 51, e2023GL107680. <https://doi.org/10.1029/2023GL107680>

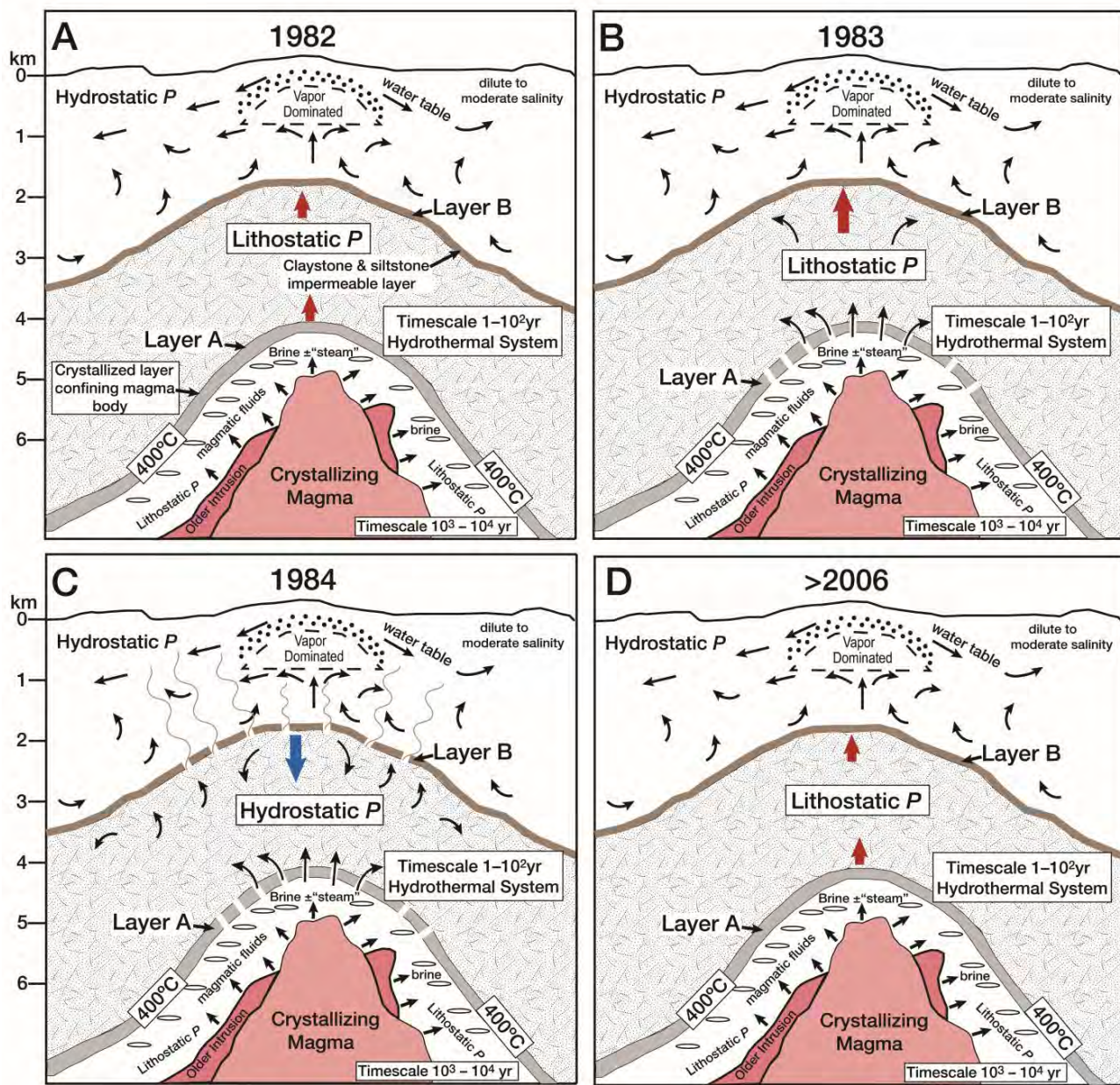
- 342 Todesco, M., and Berrino, G. (2005). Modeling hydrothermal fluid circulation and gravity signals at the Phlegraean Fields
343 caldera. *Earth and Planetary Science Letters*, 240, 328-338.
- 344 Tramelli, A., Giudicepietro, F., Ricciolino, P., and Chiodini, G. (2022). The seismicity of Campi Flegrei in the contest of an
345 evolving long term unrest. *Scientific Reports* 12, 2900. <https://doi.org/10.1038/s41598-022-06928-8>.
- 346 Troise, C., De Natale, G., Schiavone, R., Somma, R., and Moretti, R. (2019). The Campi Flegrei caldera unrest: discriminating
347 magma intrusions from hydrothermal effects and implications for possible evolution. *Earth Science Review*, 188, 108-122.
- 348 Woo, J.Y.L., Kilburn, C.R.J., 2010. Intrusion and deformation at Campi Flegrei, southern Italy: Sills, dikes, and regional
349 extension. *Journal of Geophysical Research: Solid Earth*, <https://doi.org/10.1029/2009JB006913>.
- 350 Vanorio, T., and Kanitpanyacharoen W. (2015). Rock physics of fibrous rocks akin to Roman concrete explains uplifts at
351 Campi Flegrei Caldera. *Science*, 349, 6248, 617-621.
- 352 Zollo, A., Maercklin, N., Vassallo, M., Dello Iacono, D., Virieux, J., Gasparini, P. (2008) Seismic reflections reveal a massive
353 melt layer feeding Campi Flegrei caldera. *Geophys Res Lett* 35. doi:10.1029/2008GL034242
- 354
- 355



356

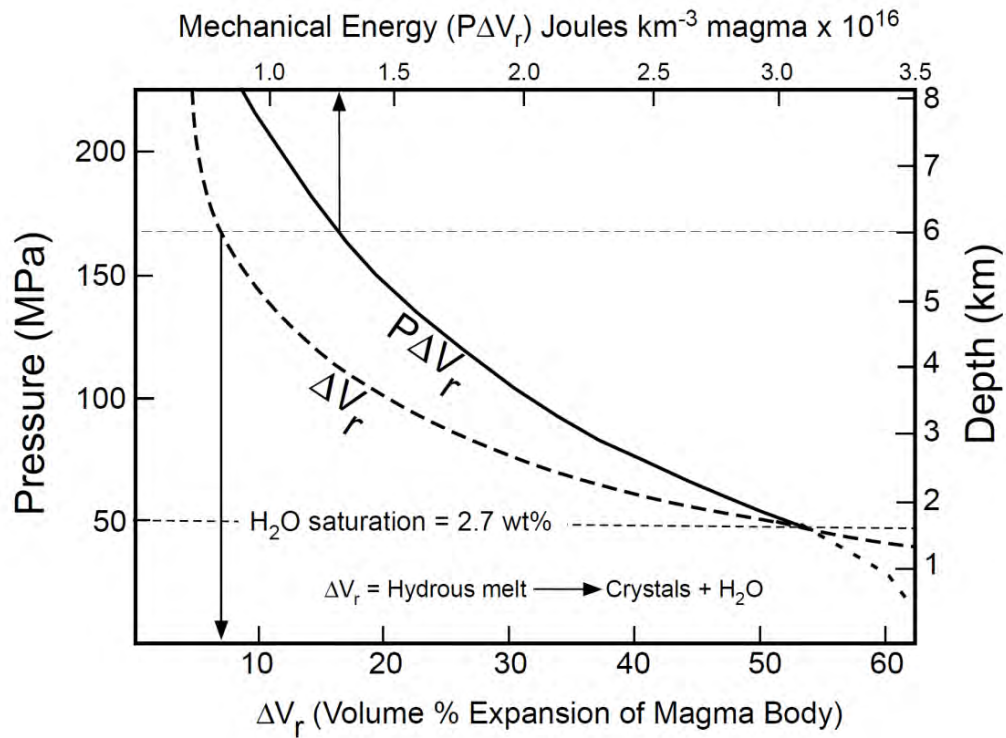
357 **Figure 1.** Map of Campi Flegrei showing the area of maximum vertical deformation (mvd), the areas of
358 decreasing vertical deformation around Pozzuoli, and locations of geothermal wells (M1, M2, M5, SV1,
359 SV3) drilled by AGIP-ENEL (AGIP, 1987) (modified from Todesco and Berrino, 2005).

360



361

362 **Figure 2.** Layer A marks the “brittle-ductile transition zone” that separates the magmatic system (at a
 363 depth > 5 km) from the overlying hydrothermal system which, in turn, is confined by impermeable layer B
 364 at a depth of about 2.5-3 km (see Lima et al. 2009 Fig. 3). When the system is closed and fluids are
 365 retained at depth, uplift as occurred in 1982 and 2005 takes place. Conversely, when brecciation occurs
 366 and fluids migrate upwards via a fracture permeability, subsidence occurs. The engine that controls
 367 bradyseism is always the deep magmatic system where heat is converted to mechanical energy by fluid
 368 expansion as shown in Figure 3 (modified from Lima et al., 2021).
 369



370
371 **Figure 3.** Volume change (ΔV_r) and mechanical energy ($P\Delta V_r$) associated with crystallization of an H₂O-
372 saturated melt and exsolution of an H₂O magmatic fluid. The calculated values assume a closed system
373 (Bodnar et al., 2007, modified after Burnham, 1972, 1985).
374